Flue gas treatment by power-to-gas integration for methane and ammonia synthesis – Energy and environmental analysis

Beatrice Castellani[a],[*], Sara Rinaldi[a], Elena Morini[a], Benedetto Nastasi[b], Federico Rossi[c]

[a] *Department of Engineering, Interuniversity Research Centre on Pollution and Environment "Mauro Felli"(CIRIAF), University of Perugia, Via G. Duranti 67, 06125 Perugia, Italy*
[b] *Department of Architectural Engineering and Technology (AE + T), TU Delft University of Technology, Julianalaan 134, 2628 BL Delft, The Netherlands*
[c] *Department of Engineering, Interuniversity Research Centre on Pollution and Environment "Mauro Felli"(CIRIAF), University of Perugia, Scientific Pole of Terni, Pentima Bassa, 05100 Terni, Italy*

ARTICLE INFO

Keywords:
Flue gas
Power to gas
CO_2 methanation
Ammonia synthesis
Carbon and energy footprint
LCA life cycle assessment

ABSTRACT

The present paper aims at assessing the carbon and energy footprint of an innovative process for carbon dioxide recycling, with flue gas as feedstock of nitrogen and carbon dioxide. Nitrogen is converted into ammonia through the Haber-Bosch process and carbon dioxide into methane via Sabatier reaction using hydrogen produced by renewable electricity excess. Carbon and energy footprint analysis of the process was assessed based on experimental data related to hydrogen production by electrolysis, methane synthesis via Sabatier reaction, energy consumption and energy output of the process units for flue gas separation, carbon dioxide methanation and ammonia synthesis. A Life Cycle Assessment method is applied, based on the experimental and computational data, both in case of renewable electricity excess and electricity from the grid. Results show that in case of renewable electricity excess, for a functional unit of 1 kg of treated flue gas, the specific carbon footprint is 0.7819 kg_{CO2eq} and energy footprint is 50.73 MJ, which correspond to 4.012 kg and 260.3 MJ per 1 kg of produced hydrogen. In case of electricity from the grid, the specific carbon footprint is 1.550 kg_{CO2eq} and energy footprint is 59.12 MJ per flue gas mass unit. If the carbon footprint is positive, the process indirectly leads to avoided emissions, ranging from 0.673 to 0.844 $kg_{CO2eq}\,kg_{fluegas}^{-1}$, thus proving the sustainability of the proposed pathway.

1. Introduction

Moving towards the implementation of the Circular Economy plan at European level drew attention to the waste and by-products of a process [1]. Resource efficiency, i.e. reducing the raw material dedicated to obtain a certain amount of product, should be coupled with the utilization of the other results of the process for increasing the yield of the process itself or to provide raw material to others. Among such options, flue gas is the by-product of fuel combustion [1]. Flue gas is composed by Greenhouse Gases (GHG), mainly carbon dioxide (CO_2) entailing negative effects on the environment. In order to comply with law in force the industry sector has to be equipped with CO_2 removal technologies [2]. Residual CO_2 may be used to produce gaseous or liquid fuels via a large number of pathways based on the transformation of renewable energy [3]. Power-to-gas (PtG) process converts electricity into hydrogen (H_2) through water electrolysis and then methane (CH_4) is produced from CO_2 and H_2 via Sabatier reaction. PtG technology is

studied with energy purposes to allow a better integration of the fluctuating renewable energy in the electric grid.

There are several pilot and demonstration plants, mainly in Europe, both for H_2 and synthetic CH_4 production, which have proven the viability of the technology [3]. PtG system variations and configurations devoted to the production of H_2 and CH_4 have been extensively studied from a technical and environmental point of view, also in combination with anaerobic digestion. Collet et al. [4] compared two biogas upgrading scenarios (with amines and membrane technologies), and three scenarios with the use of PtG technologies to produce bioCH_4 with a fossil reference one of CH_4 production from natural gas. They found that PtG technologies are competitive economically with upgrading scenarios for an average electricity price equal to 38 € MW h^{-1} for direct methanation and separation by membranes. In case of intermittent operation, competitive prices of electricity for methanation can be higher, depending on the operation time. As far as environmental aspects are concerned, results showed that impacts of PtG are higher

---

Nomenclature

Acronyms

CED	Cumulative Energy Demand
CF	Carbon Footprint
COP	Coefficient Of Performance
EF	Energy Footprint
GHG	Greenhouse Gases
GWP	Global Warming Potential
HHV	Higher Heating Value
IPCC	International Panel on Climate Change
LCA	Life Cycle Assessment
PEM	Proton Exchange Membrane
PtG	Power to Gas
PV	Photovoltaics

Chemical symbols

Al_2O_3	Aluminum Oxide

CH_4	Methane
CO_2	Carbon Dioxide
H_2	Hydrogen
H_2O	Water
HCl	Hydrogen Chloride
KOH	Potassium Hydroxide
N_2	Nitrogen
NH_3	Ammonia
Ni	Nickel
NiO_2	Nickel Oxide
NOx	Nitrogen Oxides
O_2	Oxygen
PtG	Power To Gas
SO_2	Sulfur Dioxide
Zr	Zirconium

---

than biogas upgrading for continuous operation, while intermittent operation can severely lower the environmental impact for non-direct methanation scenarios if the consumed electricity is mainly renewable. In [5] it was assessed that PtG systems are competitive economically with conventional gas production systems when other services, such as heat and oxygen supply are provided and bring environmental benefits only when supplied with renewable sources. Castellani et al. [6] studied experimentally the integration of PtG technology with hydrate-based biogas upgrading, concluding that there are benefits in terms of net energy stored, as gaseous CH_4, passing from raw biogas utilization to the integration of biogas upgrading with CO_2 methanation. The energy content improvement is 41.2%. Nevertheless, the addition of hydrogen electrolysis within the energy system boundaries brings significant energy losses. Indeed, the energy benefit is reduced to 0.1%.

Zhang et al. [7] compared the environmental performance of PtG with conventional H_2 and natural gas production and utilization. They found that the best option in terms of GHG emission reduction is renewable electricity supply coupled with biogenic CO_2 sources.

A new research line related to the so-called synthetic fuel started with CO_2 sequestration from flue gas and its reaction with H_2 to produce methanol [8,9] by combining the GHG emission reduction with the use of renewable electricity excess due to the increase of the intermittent renewable energy supply or even combined with other waste heat such as in [10]. This synergy is extended to inter-sectorial systems [11] and multiple fuels production [12] for feeding power plants or producing further raw material in industrial processes.

In this perspective, H_2 from renewable energy can be used to produce chemicals, such as ammonia (NH_3), in addition to CH_4·NH_3 is produced conventionally via the Haber-Bosch process, which combines H_2 from steam reforming of natural gas and nitrogen (N_2) from cryogenic air separation. In the literature, several studies show Life Cycle Assessment (LCA) of various NH_3 production paths: biomass gasification [13], municipal waste, hydropower and nuclear energy for H_2 production [14].

The present paper proposes flue gas as a source of reactants, both for synthetic CH_4 and NH_3 production. Flue gas is a gaseous industrial waste, composed mainly by N_2 and CO_2. N_2 and CO_2 constitute feedstock for NH_3 and CH_4 production, respectively, if combined with H_2. Considering the state of art, this is the first study in the literature on the flue gas treatment process for the NH_3 production via Haber-Bosch synthesis and the CH_4 production via Sabatier reaction in combination with electrolysis for H_2 production. The proposed integrated process addresses a double challenge: (i) recycling of an industrial waste, such

as flue gas, and its conversion into a CO_2/N_2 source for high-value products, CH_4 and NH_3 and (ii) utilization of renewable energy for H_2 production as an energy storage option.

The Energy Footprint (EF) and the Carbon Footprint (CF) will be assessed with the support of experimental data as analyzed by some of the authors in a previous study [15], in which an environmental assessment is performed to evaluate the production of methane from hydrate-based biogas upgrading coupled with PtG technology. The CF and EF are evaluated to understand the impact of the proposed solution, in terms of GHG emissions and primary energy consumption. The results are presented and compared with traditional production processes.

2. Methods

The treatment process of flue gas, consisting of four main phases, is described in the following section. Deriving from the deep analysis of the process and experimental tests, the energy balance and environmental assessment are computed.

2.1. Process description

The proposed process treats flue gas, the final gaseous product of combustion, to produce CH_4 and NH_3 through renewable energy excess exploitation. For their composition, flue gases from fossil fuel-fired combustion facilities are major contributors to atmospheric pollution [16]. The composition of flue gases depends on the fuel source, the power plant and treatments; however, they generally consist of CO_2, N_2, oxygen (O_2) and water (H_2O), sulfur dioxide (SO_2), nitrogen oxides (NO_x) and hydrogen chloride (HCl). For the purposes of the investigation, a flue gas composed by CO_2 and N_2 is considered. Previous stages of purification are not taken into account.

CO_2 and N_2 from flue gas are separately combined with H_2 in the Sabatier reaction to produce CH_4 and in the Haber-Bosch process to produce NH_3, respectively. The overall process is shown in Fig. 1.

The separation of CO_2 and N_2 is carried out by silicone hollow fiber membrane technology. The H_2 that is required to realize the Sabatier reaction and the Haber-Bosch process is provided by electrolysis of water [17] based on renewable energy excess use.

CO_2 and H_2 are combined by Sabatier reaction, with a stoichiometric ratio of 1:4 and produces CH_4 and water exothermically as shown in Eq. (1):
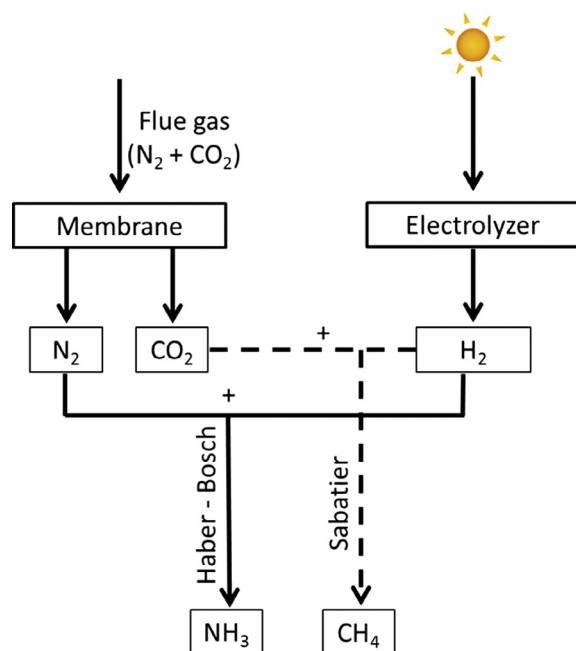
$$CO_2 + 4H_2 \leftrightarrows CH_4 + 2H_2O \tag{1}$$

Fig. 1. Scheme of the combined processes to produce NH_3 and CH_4 from flue gas.

N_2 is combined with H_2 in accordance with the Haber-Bosch process, with a stoichiometric ratio of 1:3 and in presence of a catalyst based on magnetite. The chemical reaction for NH_3 production is shown in Eq. (2):

$$N_2 + 3H_2 \leftrightarrows 2NH_3 \qquad (2)$$

Methane and ammonia are stored in the gaseous form.

In the following sub-sections, the considered processes are described.

2.1.1. Carbon dioxide/Nitrogen separation

Various technologies are used for post-combustion CO_2 separation: absorption with solvents or solid sorbents, pressure and temperature swing adsorption with several solid sorbents, cryogenic separation, membranes and other several emerging technologies. Among these ones, clathrate hydrates are widely studied in the last few years [18]. In accordance with reviews in the literature, membranes will be significantly more efficient at separation than liquid absorption soon, which is currently considered the most promising method [19]. In addition, membranes have several advantages over conventional separation techniques, such as low environmental impact, favorable economics, ease of operation, and low maintenance [20]. Several typologies of membranes are available for CO_2 separation purposes: polymeric and inorganic membranes, mixed matrix membranes, facilitated transport membranes and carbon membranes. A comprehensive list of membranes and their permeability to CO_2 and N_2 is available in [21]. According to [22], a polymeric gas separation membrane guarantees the separation of CO_2 from other gases, a good permeation to the gas to have an intense gas flux during separation, as well as good thermal and mechanical properties. In the present paper, the selected membrane module is constituted by hollow fibers, which are small silicone micro-tubes with very thin walls (supplied PermSelect®). Technical data are shown in Table 1.

Hollow-fiber membranes have a higher productivity in the processes of separation, since they provide high area-to-volume ratio, low resistance to gas flow and the ability to support high transmembrane pressure drops [23]. Since silicone is dense, the separation occurs because of the permeability difference between gases in the fibers. The permeability coefficient is a parameter defined as the transport flux of a

gas (rate of gas permeation per unit area), per unit transmembrane driving force per unit membrane thickness [24]. The permeability coefficient, at 298 K and 0.1 MPa, for N_2 is 280 barrer while for CO_2 it is 3250 barrer [25]. The separation factor, calculated as the ratio between the two permeability coefficients is equal to 11.6 and this value in accordance with technical data by the supplier ensures an excellent separation. The N_2/CO_2 mixture enters the membrane module through the inlet port to the tube side and flows through the inside of the hollow fibers. CO_2 has the highest permeability and so transfers across the hollow fiber walls leaving behind N_2. The transferred gas is referred to as the permeate (in this case the permeate is CO_2). Exiting the outlet of the tube side is the retentate, which constitutes a gas mixture with a higher concentration of N_2.

According to both [26,27], the trade-off between permeability and selectivity limits the achievement of simultaneous high degree of CO_2 separation and high CO_2 purity with a one single-stage membrane. To reach 90% CO_2 separation and a 95 mol% CO_2 purity, a two-stage membrane section with recirculation is considered, as shown in Fig. 2.

The separation section, shown in Fig. 2, uses a compressor at 0.4 MPa for the feed flue gas and a vacuum pump at 0.01 MPa. Energy calculations on this configuration are presented in [28] and energy consumption is equal to 878.4 kJ_{el} per mass unit of separated CO_2. In accordance with [28], this value is consistent with energy consumption of ammine-based process, which is the most used carbon capture technology.

2.1.2. Hydrogen production

Water is decomposed into O_2 and H_2 by an electric current being passed through the water. The electrolysis of one mole of water produces a mole of H_2 gas and a half-mole of O_2 gas in their normal diatomic forms. Two moles of water undergo the transformation in Eq. (3):

$$2H_2O + \text{electrical energy} \rightarrow O_2 + 2H_2 \qquad (3)$$
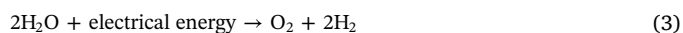
Three water electrolysis technologies are widely investigated: alkaline electrolysis, Proton Exchange Membrane (PEM) electrolysis and solid oxide electrolysis. For large-scale applications, the most used water electrolysis technology is the alkaline process, while PEM technology is less mature than the alkaline one and is mostly used for small-scale applications [29]. Solid oxide electrolysis is the least developed process and it is not yet widely commercialized [30]. The electrolyzer used in the experimental tests is based on PEM technology and is supplied by Erre Due Srl (H03 series). Technical characteristics of the electrolyzer are shown in Table 2. The energy efficiency, defined as the Higher Heating Value (HHV) of H_2 divided by the energy consumed by the electrolysis system per kg of H_2, is equal to 57.4%.

The electrolyzer was put in operation in 2005 and its power consumption is quite high with respect to other devices in the market. As a matter of fact, several studies in the literature show that power consumption can reach values of 15480 kJ per Nm^3 of H_2 for alkaline technology and 14760 $kJ\ Nm^{-3}$ for PEM technology [31]. A reduction of 10% on the alkaline electrolysis energy consumption was observed when compounds of three d-metals (ZnCoMo) were added to the standard potassium hydroxide (KOH) solution [32]. Commercial alkaline electrolyzer, supplied by Nel Hydrogen, has: (i) a declared power

Table 1
Membrane module characteristics and operating conditions.

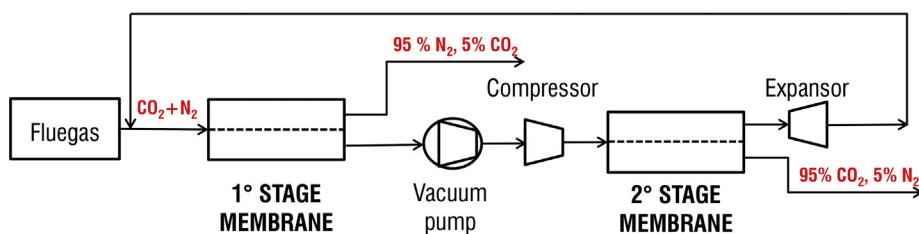| Parameter	Value/typology
Membrane material	PDMS (Silicone)
Membrane type	Dense Hollow Fiber
Fiber ID (μm)	190
Fiber wall thickness (μm)	55
Max continuous operating temperature (K)	333
Max shell side pressure (MPa)	1.5
Typical gas flow rate ($Nm^3\ h^{-1}$)	3.9

Table 2
Electrolyzer technical data.

Parameter	Value
Operating pressure (MPa)	0.25
Flow rate (Nm^3 h^{-1})	2.5
Power consumption (MJ Nm^{-3})	21.6

consumption down to 13680 kJ Nm^{-3} (in the range of 13680–15840 kJ Nm$_{H2}^{-3}$) with a 78–90% energy efficiency and (ii) a water consumption of 0.9 L per Nm^3 of produced H$_2$, with a water-to-hydrogen conversion efficiency of 89% [33].

2.1.3. Methane production

The Sabatier reaction, used for CH$_4$ production from CO$_2$, is exothermic ($\Delta H° = -165$ kJ mol^{-1}) and occurs within the optimal temperature range 523–673 K, in order to guarantee a higher CO$_2$ conversion and, consequently a higher CH$_4$ selectivity. Heat produced by the exothermic reaction is, thus, removed to maintain a relatively low process temperature (around 623 K). Pressure is directly proportional to H$_2$ conversion and its effect is improved at higher temperatures, where the equilibrium constant is low. The methanation of CO$_2$ is thermodynamically convenient ($\Delta G_{298K} = 113.5$ kJ mol^{-1}). However, the reduction of the fully oxidized carbon to CH$_4$ is an eight-electron process with important kinetic limitations. Therefore, a catalyst is used for reaching acceptable rates and selectivity. Nickel was the first catalyst used when Paul Sabatier discovered this process in 1897 and it is still commonly used due to its availability and relative low cost. A support with high surface area, usually oxides, has been applied extensively for the preparation of metal catalysts. The most widely used reactor design for methanation processes is the fixed bed reactor.

The CO$_2$ methanation process was studied experimentally through the operation of a lab-size apparatus. The schematic diagram is shown in Fig. 3.

The apparatus is composed of an electrolyzer for H$_2$ production from Photovoltaic (PV) system, a CO$_2$-H$_2$ mixing section, a heating section, a Sabatier reactor and a water separation section. H$_2$ from the electrolyzer is mixed with CO$_2$ from gas bottles in stoichiometric proportion. The gaseous mixture passes in the heating section, which is a horizontal tube (diameter of 25.4 mm and length of 300 mm) equipped with three 700 W mineral insulated band heaters, provided by Watlow. The heating section is connected to the Sabatier reactor through a gate valve (supplied by Swagelok, model SS-6nbs 10 mm-G). The Sabatier reactor is a cylindrical AISI 304 stainless monotubolar fixed bed reactor (diameter of 25.4 mm and a length of 300 mm). It is filled with nickel (Ni) catalyst pellets.

Finally, the reaction products go to the water separation section, constituted by a 6 mm stainless steel cooling coil, immersed in a thermostatic bath. In this section, water vapor condensation occurs and the gaseous incondensable products are collected for gas chromatographic analysis. The gaseous mixture flow rate is 0.63 m^3 h^{-1}. The installation of the apparatus is shown in Fig. 4. Gas flows are measured and controlled by flowmeters, supplied by Bronkhorst (El-flow Series), with the following characteristics: flow rate in the range from 0.08 to 4 Nm^3/h; maximum inlet pressure 3 MPa; control stability lower than ± 0.1% FS

and temperature sensitivity lower than 0.05% FS/K.

The two cameras are provided with temperature and pressure sensors:

- bourdon tube pressure gauge (NG100 series) supplied by Kobold (accuracy class 1), with a pressure range from 0 to 4 MPa;
- mineral insulated type K thermocouples (accuracy class 1).

Voltage signals from pressure transducers and temperature sensors are collected by a software for data acquisition on a personal computer. Pressure and temperature data are collected every 5 s. Gas chromatographic analyses are carried out with a gas chromatographer supplied by VARIAN (model VARIAN CP 4900 Micro-GC). Measurements, periodically carried out with certified mixtures, show that uncertainties are always lower than 1%, with an excellent repeatability on sequences of samples [18].

The Sabatier reaction is catalyzed by Ni-based catalyst supplied by BASF (G1-85 T5x5). BASF G1-85 Ni/Zr/Al$_2$O$_3$ catalyst contains metallic nickel and zirconium on an aluminum oxide support: the nickel content in weight is 50%. It is supplied in 1 mm × 4 mm cylindrical pellets, with a specific surface area of 123 m^{2}g^{-1}. The nickel oxide (NiO) is converted into the catalytically active form for the methanation reaction through an activation process described in [9]. Gas bottles were supplied by Air Liquide Italia Service. The purity of CO$_2$, N$_2$ and H$_2$ used in the CO$_2$ methanation process for catalyst activation is 99.999%.

Three tests were carried out continuously using a stoichiometric H$_2$/CO$_2$ ratio equal to 4 (H$_2$ volume fraction and CO$_2$ volume fraction equal to 80% and 20%, respectively) and with an hourly space velocity (the ratio between the flowrate and the reactor volume) of 413 h^{-1}. Experimental tests were carried out with an initial internal temperature near to 673 K and an initial internal pressure from 0.2 MPa to 2 MPa. Table 3 shows temperature and pressure values (referred to the internal initial conditions and measured inside the reactor at the steady state), final volume fractions in the gaseous mixture and CO$_2$ conversion efficiency. The reaction time, which is considered to start from the temperature increase, was equal to 30 min for all the tests.

The CO$_2$ conversion increases with pressure. Test at 2.0 MPa and at
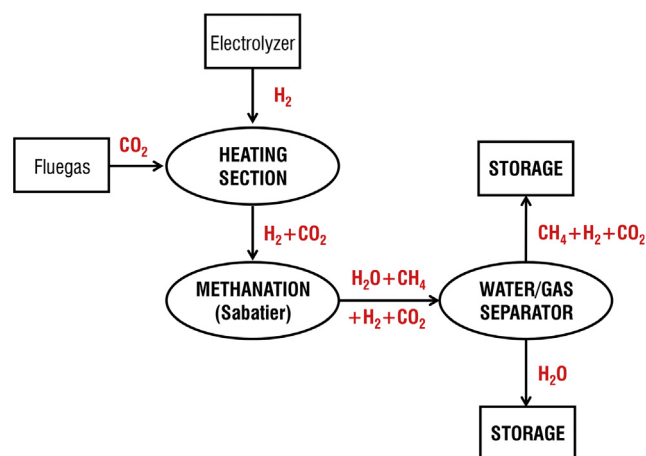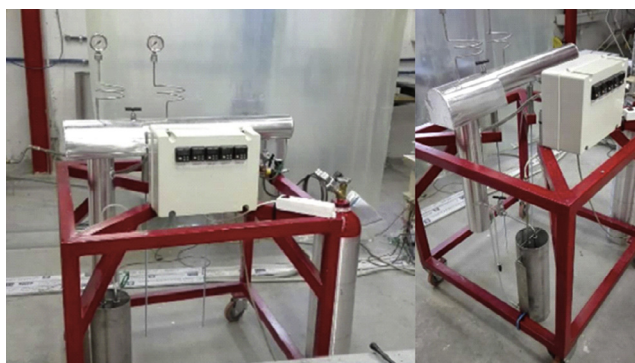

Fig. 3. Methanation process.

Fig. 4. Experimental apparatus for CO_2 methanation process: (a) front view; (b) side view.

Table 3
Test conditions for CO_2 methanation.

Test	Pressure [MPa]	Temperature [K]	Final % v/v			CO_2 conversion efficiency [%]
			H_2	CH_4	CO_2	
1	0.2	690	26.52	65.70	7.78	64.58
2	1.0	675	24.58	64.75	3.95	80.25
3	2.0	694	2.68	96.43	0.89	95.55

an internal temperature of 694 K, with a stoichiometric CO_2/H_2 ratio shows a CO_2 conversion equal to 95.55%.

2.1.4. Ammonia production

NH_3 has a number of favorable attributes both as H_2 carrier if compared to other H_2 storage materials and as fuel. First of all, NH_3 has a high capacity for H_2 storage (about 17.7% stoichiometric content of H_2) [14]. Furthermore, the NH_3 production is based on a very well-known process, and technologies and plants for a large scale NH_3 production and distribution are already available [34]. Comparing NH_3 with H_2 and various other fuels, it can make sense to store H_2 as NH_3, characterized by an energy content equivalent to 21.23 MJ kg^{-1}. Another important aspect of NH_3 is that it contains no carbon. Therefore, when ammonia-based fuel is burned, it produces lower greenhouse gases emissions.

Technologies for ammonia storage are also well-developed. NH_3 is a compound with relative stability, liquid at 288 K and with a vapor tension of 0.6 MPa. It liquefies at ambient temperatures at about 1.0 MPa or at 240 K at 0.1 MPa; it is also stored as liquid solution with water. It has decreasing solubility in solvent liquids as the temperature of the solvent increases; at 288.6 K, the density of a saturated solution is 880 kg m^{-3} and contains 35% NH_3 by mass. In general, three methods of storage of liquid NH_3 are currently used: at ambient temperature and equivalent pressure, under pressure in spherical vessels, and at atmospheric pressure at 240 K. The choice depends primarily on the quantity of liquid NH_3 to store, the economic aspect and the end use. In this study, NH_3 was considered compressed at about 1.0 MPa.

The Haber-Bosch reaction used for NH_3 production from N_2 and H_2 is highly exothermic and produces 92 kJ mol^{-1}. Optimal values of temperature and pressure are included respectively between 623 and 823 K and 14–32 MPa. High temperatures are necessary to split the bi-nitrogen molecule, or to break triple bond existing between the two nitrogen atoms. In this way, kinetics of the separation reaction is accelerated but at the same time, this value of temperature makes the synthesis reaction more complicated. The most widely used catalyst is iron, because of its availability and its low cost.

Aluminum oxides are added to the catalytic mixture to protect the catalyst and to hinder this process. The industrial process is composed of several steps. H_2 and N_2 are compressed to reach the optimal value,
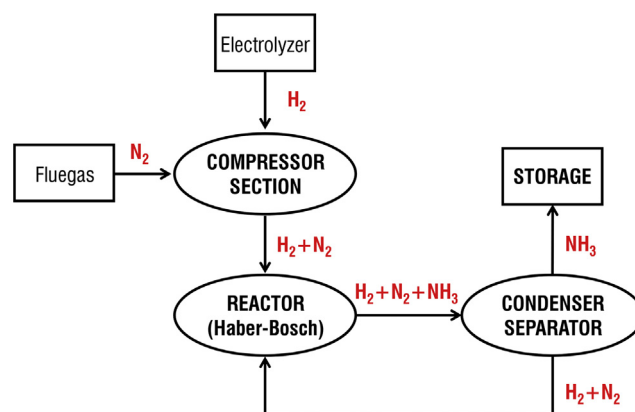

Fig. 5. Scheme of Haber-Bosch process.

and then they are sent to the reactor where the heater heats them to the right temperature and catalysts work for NH_3 production. At the exit of the reactor, there is NH_3, and also unreacted H_2 and N_2. This mixture goes to a heat exchange, which separates a part of unreacted reagents and sends them to the reactor. The other part of the mixture has a high NH_3 percentage and reaches a capacitor in order to obtain pure NH_3. The remaining part of reactants is compressed a second time and sent to the heat exchanger, then to the reactor. The produced NH_3 is then stored. The process units are shown in Fig. 5. A recycling loop is generally used since single-stage reactant conversion is very low and equal to 15–20% [35]. Improved Haber-Bosch plant configurations have been proposed based on the integration with biogas or gasification plants [36].

Current industrial NH_3 plants use H_2 production processes, steam/air reforming and partial oxidation process. The type of feedstock used plays a significant role in the consumed energy amount and in the produced CO_2. The steam reforming of natural gas produces 2.1 kg$_{CO2}$ kg$_{NH3}^{-1}$, while in partial oxidation the emissions are in the range 3.3–4.6 kg$_{CO2}$ kg$_{NH3}^{-1}$ depending on the feedstock. According to literature studies, the average energy consumption in 93 NH_3 plants was 36.6 MJ kg$_{NH3}^{-1}$ [37].

2.2. Energy and environmental evaluation

In the following subsections, the energy balance of the process and the method for energy and carbon footprint analysis are detailed.

2.2.1. Energy balance

Flue gas was assumed to be a gas mixture of CO_2 and N_2 (20% in volume of CO_2) at 293 K and 0.1 MPa [38]. 1 kg of flue gas is constituted by 25.6 mol of N_2 and 6.4 mol of CO_2. For CO_2/N_2 separation, a two-stage membrane separation process with a CO_2 purity of 95% and a CO_2 separation degree of 90% was considered. The specific energy consumption was calculated in [39] and is equal to 878.4 kJ$_{el}$ kg$_{CO2}^{-1}$. Considering the composition of the flue gas, the energy consumption is equal to 235 kJ$_{el}$ kg$_{fluegas}^{-1}$. After separation, which is assumed to ensure 90% CO_2 separation and a 95 mol% CO_2 purity, 6.1 mol of CO_2 at 0.4 MPa are used for the Sabatier reaction and 24.4 mol of N_2 are used for the Haber-Bosch reaction. H_2 is produced by electrolysis of water. The H_2 moles necessary for Sabatier reaction and NH_3 production are calculated using the stoichiometric proportions and are equal to 97.4 moles$_{H2}$ kg$_{fluegas}^{-1}$. Energy consumption for the electrolysis is equal to 13680 kJ Nm$_{H2}^{-3}$ as in [33]. Energy costs related to the methanation process consist of:

- H_2 and CO_2 compression for injection into the synthesis reactor,
- energy consumption for reactor's heating to the synthesis temperature,

- removal of reaction heat.

To assess the above cited contributions, the following assumptions were made. H_2 is compressed to 0.4 MPa and then mixed with CO_2 from the separation section. The gaseous mixture is compressed from 0.4 MPa to 2.0 MPa, with an initial temperature of 293 K, through a single stage compression. The following efficiencies were considered: isentropic efficiency equal to 0.85, mechanical efficiency equal to 0.93 and electrical efficiency equal to 0.98. The H_2/CO_2 mixture is heated to 724 K from the final compression temperature of 408 K in order to reach the operating conditions. Heating is assumed to be carried out by band heaters as in Section 2.1.3; the energy conversion efficiency is assumed equal to 0.75 to take into account heat losses. Sabatier reaction is an exothermic process, with an enthalpy of formation of 165 kJ mol^{-1}. Reaction heat is considered to be removed through a cooling process with a coefficient of performance (COP) equal to 3. Water-methane separation is not considered since it occurs at environmental temperature. For the NH_3 production, N_2 is mixed with H_2 with 1:3 stoichiometric ratio. As for the methanation section, energy costs consist of H_2 and N_2 compression, heating to the synthesis temperature and removal of reaction heat and the same assumptions were considered for the calculation. The mixture is considered to be compressed to 25 MPa with a four-stage compression with intercooling. The mixture is then heated to 823 K. The reaction heat, equal to 45.64 kJ mol^{-1} is removed with a chiller with a COP equal to 3. NH_3 separation is a condensation process, whose energy consumption is considered equal to zero. The analyzed energy costs are summarized in Table 4.

The total energy consumption per mass unit of flue gas is equal to 36,328 kJ$_{el}$, which corresponds to 186,418 kJ$_{el}$ per unit mass of H_2. The electrolysis covers almost 80% of the electrical energy costs. The corresponding primary energy need, considering a conversion factor of 0.46, is 78973 kJ kg$_{fluegas}^{-1}$ equal to 405,256 kJ$_{el}$ kg$_{H2}^{-1}$. The electric energy/primary energy conversion factor is related to the Italian energy scenario and determined by the Italian authority ARERA [40].

The investigated process produces 5.8 mol (0.166 kg) of CH_4 and 9.7 mol (0.092 kg) of NH_3 (Table 5). The conversion of a mass unit of H_2 leads to 0.475 kg of CH_4 and 0.850 kg of NH_3. To calculate the energy output, the following considerations were made. For the Sabatier reaction, the experimental conversion efficiency, obtained in Section 2.3 and equal to 95%, was considered. For the NH_3 production, the conversion efficiency was assumed equal to 20%, as found in the literature [41]. For both processes, calculations refer to a single-stage process without reactant recirculation. Since heat of combustion is equal to 50000 kJ kg^{-1} and 18480 kJ kg^{-1} for CH_4 and NH_3, respectively, the energy output for mass unit of flue gas is 7684 kJ (Table 5). The energy output for mass unit of H_2 is 39433 kJ.

2.2.2. Carbon and energy footprint method

The life-cycle CF and EF are performed with the SimaPro® v8.4.0.0 software [42] in accordance with ISO/TS 14,067 [43] and the ISO 14,040 series [44]. The standard CF method IPCC 2013 GWP 100a within the SimaPro software is used [42]; the quantification is based on the activity data multiplied by appropriate emission factors that quantify CO_{2eq} emissions per unit activity. The GHG emissions associated to the i-th process (CF_i) is computed using equation (4):

$$CF_i = EF_i \cdot A_i \qquad (4)$$

where A_i is the activity data and EF_i is the emission factor of the i-th process, respectively.

The life-cycle primary energy consumption is also computed selecting the Cumulative Energy Demand (CED) assessment method. The CED of a product or system throughout the entire life cycle includes both the direct and indirect energy use, allowing the calculation of the EF. This enables the evaluation of the primary energy consumption and the GHG emissions associated to the flue gas treatment process for the production of NH_3 via Haber-Bosch synthesis and the production of CH_4

via Sabatier reaction starting from flue gas separation.

The LCA analysis was carried out in accordance with a cradle-to-gate approach, considering input material and production phases of a ready-to-use gas. The reference functional unit is 1 kg of flue gas treated in input, but results will be presented also for 1 kg of H_2 used. The system boundaries, given in Fig. 6, are focused on all the processes and materials required to convert flue gas into CH_4 and NH_3. In particular, they include the production of input materials (i.e. reagents, water, catalyst, and membrane), and the production of energy required by separation, electrolysis, methanation and ammonia synthesis processes. The boundaries do not include the energy conversion of the CH_4 and NH_3 produced. A mass allocation was used to evaluate the impact, in terms of energy and GHG emissions, of the different phases of the process.

The energy needs for the process steps are supplied by a renewable multicrystalline PV system. The solar technology was determined on the basis of its CF. In accordance with Ecoinvent database within SimaPro Software [42], multicrystalline silicon solar cells have a CF of 20.5 kg$_{CO2eq}$ per GJ produced, while single crystalline silicon solar cells have a CF of 24.2 kg$_{CO2eq}$ per GJ produced. To study also the case in which the renewable electricity excess is not available, the LCA analysis was carried out also for the case of the electricity supply from the grid.

Inventory data referred to 1 kg of flue gas treated are shown in Table 6. For the evaluation of the amount of membrane and catalyst necessary for the treatment of 1 kg of flue gas, the lifetime and the annual working hours were considered.

To quantify the membrane needed to treat 1 kg of flue gas, a lifetime of 10 years, a total weight of 0.475 kg, 700 h y^{-1}, and a flow rate 3.6 Sm^3 h^{-1} are considered.

In Table 6 process energy needs are covered by electricity. Electricity is used for reactants' compression and heating and for removal of reaction heat. For CO_2 methanation, inventory data are based on the configuration and operation of the experimental apparatus in which heat is supplied by electrical band heaters. In industrial plants, heat recovery allows to obtain much more efficient configurations: the heat of the methanation reaction, for instance, could be used for the regeneration of scrubbing liquids or sorbents in the CO_2 separation section or, alternatively, for pre-heating reactants.

Electricity input in ammonia industrial plants is not used, as most of NH_3 production is based on steam reforming in which heat recovered from the primary reformer flue gas is used to produce high pressure steam used to drive synthesis gas, process air and refrigeration compressors [45]. In addition, gases from reforming sections, before entering the synthesis reactor, are already at high temperature. Heat needs are generally supplied by burning natural gas or other gaseous fuel. This configuration is not consistent with the presented process, in which steam reforming is replaced by water electrolysis.

Table 4
Energy input for CO_2 methanation and NH_3 production.

Energy input			
Process	Energy consumption	(kJ$_{el}$ kg$_{fluegas}^{-1}$)	(kJ$_{el}$ kg$_{H2}^{-1}$)
N_2/CO_2 separation	Membrane separation	235	1208
H_2 production	Electrolysis	29,839	153,120
CO_2 methanation	Compression	1498	7686
	Gas mixture heating	1354	6947
	Reaction heat removal	318	1631
NH_3 synthesis	4-stage compression	1625	8341
	Gas mixture heating	1384	7104
	Reaction heat removal	74	380
Total energy consumption		36,328	186,418

Table 5
Energy output for CO_2 methanation and NH_3 production.

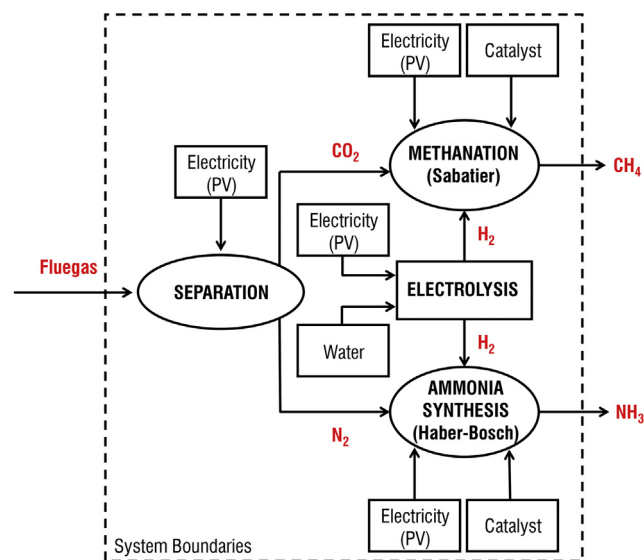| Product	Energy output				
	Amount (mol $kg_{fluegas}^{-1}$)	Amount (kg $kg_{fluegas}^{-1}$)	Amount (kg kg_{H2}^{-1})	Energy content (kJ $kg_{fluegas}^{-1}$)	Energy content kJ kg_{H2}^{-1})
CH_4	5.8	0.092	0.475	4623	23,725
NH_3	9.7	0.166	0.850	3061	15,708

Fig. 6. System boundaries.

Table 6
Inventory data for the treatment of 1 kg of flue gas.

Phase	Input	Unit	Amount	Data source
Flue gas separation	Membrane	kg	1.03E−05	Computational data
	Electricity	kJ	235	Computational data
CO_2 methanation	H_2	kg	0.04871	Experimental data
	Electricity	kJ	3169	Experimental data
	Catalyst	kg	7.69E−05	Experimental data
NH_3 synthesis	H_2	kg	0.1461	Computational data
	Electricity	kJ	3084	Computational data
	Catalyst	kg	1.04E−05	Computational data

3. Results and discussion

Results of the LCA analysis show that, considering 1 kg of flue gas as functional unit of the study, CF and EF are 0.7819 kg_{CO2eq} kg^{-1} and 50.73 MJ kg^{-1}, respectively. The process is formed by two sections: CO_2 methanation and NH_3 synthesis via Haber-Bosch reaction. The obtained results were calculated on the basis of experimental data for the methanation process and on numerical calculations for the NH_3 section, in which a conversion efficiency of 0.2 without recirculation was considered. The estimate of the process footprint is performed considering that the electric energy, consumed within the process, is produced by PV. Fig. 7 shows the network view referred to the process that used electricity excess from renewable energy (in this case from PV).

A detail of CF analyses, when the required electricity is supplied by PV system, is given in Table 7. It can be noted that most of the environmental impact (approx. 99.8%), in terms of GHG emissions, comes from energy consumption (Fig. 7). In particular, H_2 electrolysis is responsible for 82% of the energy consumption.

From data in Table 7, the CO_2 methanation process is responsible for 29.48% of CF (0.2305 kg_{CO2eq} $kg_{fluegas}^{-1}$) and 29.45% of EF (14.94 MJ $kg_{fluegas}^{-1}$), respectively. The produced CH_4 is equal to 0.092 kg (Table 5), corresponding to 0.129 Nm^3. For the CO_2 methanation process, the CF and EF associated to the electricity from the solar renewable source are 8.71% and 8.72%, respectively. From values in Tables 5 and 7, the emitted CO_2 per GJ of energy from the combustion of the produced CH_4 is equal to 49.7 kg_{CO2eq} GJ^{-1}, which is much lower than that calculated in [5] (112.7–118.9 kg_{CO2eq} GJ^{-1}). This range is referred to a CO_2 methanation process with different electrolyzer sizes from 25 kW to 1000 MW and with CO_2 supply from direct atmosphere capture.

The NH_3 synthesis process is responsible for 70.52% of CF (0.5514 kg_{CO2eq} $kg_{fluegas}^{-1}$) and 70.55% of EF (35.79 MJ $kg_{fluegas}^{-1}$). The produced NH_3 is equal to 0.166 kg $kg_{fluegas}^{-1}$. This value is very low because of the conversion efficiency assumed to be 0.2. In real processes, with the presence of recirculation of unreacted N_2/H_2, the conversion efficiency reaches value up to 0.9. Considering that the PV electricity consumption for the NH_3 process has a very low impact on the overall CF and EF (8.47% and 8.49% respectively), an advanced production process with recirculation could be performed in order to reach higher NH_3 production. In this case, the amount of produced NH_3 would be 0.745 kg $kg_{fluegas}^{-1}$ and CF would be 0.740 kg_{CO2eq} kg_{NH3}^{-1}. The CF of the process is much lower than data for NH_3 production via traditional process, which show a CF in the range from 2.1 to 4.6 kg_{CO2eq} kg_{NH3}^{-1}, as reported in Section 2.1.4.

Comparing data of the methanation and the NH_3 production processes, in both cases the weight of the PV electricity for process stages on the overall CF and EF is much lower than the consumed electric energy for H_2 electrolysis, which results as the most energy-consuming section of the process. Despite this, producing H_2 through the use of renewable solar energy becomes an important technological path for renewable energy storage, which helps in reducing fluctuation in electricity production and increasing grid production-demand balance in temporal and spatial dimensions.

To include also the case in which the renewable electricity excess is not available, a further analysis was computed for a system using the electricity from the grid, considering the production mix for Italy. Results are summarized in Table 8.

In case of energy supply from the grid, the CF is 1.550 kg_{CO2} and the EF is 59.12 MJ per kg of flue gas, which correspond to 7.954 kg_{CO2} and 303.4 MJ per kg of H_2 produced. Using the electricity from the grid leads to a double value of CO_2 emissions with respect to the case of completely renewable energy use. The specific EF changes from 50.73 MJ to 59.12 MJ, with a 14% increase.

In the face of a positive CF, the integrated production of synthetic CH_4 and NH_3 from flue gas indirectly leads to avoided emissions, which should be accounted. Firstly, flue gas is not released in the atmosphere but converted into valuable products. The CO_2 in a flue gas mass unit, not emitted into the atmosphere, is equal to 0.282 mol.

The synthetized CH_4 replaces that produced from fossil sources, while the produced NH_3 replaces that produced from traditional processes. In accordance with literature data and Ecoinvent 3.3 database within SimaPro® v8.4.0.0 Software [42], natural gas production at extraction has a CF equal to 0.0.444 kg_{CO2eq} Nm^{-3}, while NH_3 production emissions ranges from 1.99 kg_{CO2eq} kg_{NH3}^{-1} for a steam reforming process to 3.02 kg_{CO2eq} kg_{NH3}^{-1} for a partial oxidation process. In addition, the avoided carbon emissions related to CH_4 production (0.092 kg) are equal to 0.061 kg_{CO2eq} $kg_{fluegas}^{-1}$ and those related to the NH_3 production (0.166 kg) range from 0.330 to 0.501 kg_{CO2eq} $kg_{fluegas}^{-1}$, with an average value of 0.415 kg_{CO2eq} $kg_{fluegas}^{-1}$. The total amount of the avoided CO_2 emissions ranges from 0.673 to 0.844 kg_{CO2eq} $kg_{fluegas}^{-1}$ with an average value of 0.758 kg_{CO2eq} $kg_{fluegas}^{-1}$.

It can be stated that, in case of renewable energy excess use, the flue gas treatment path globally constitutes a carbon-neutral process, and even results in estimated negative balance values, thus proving the
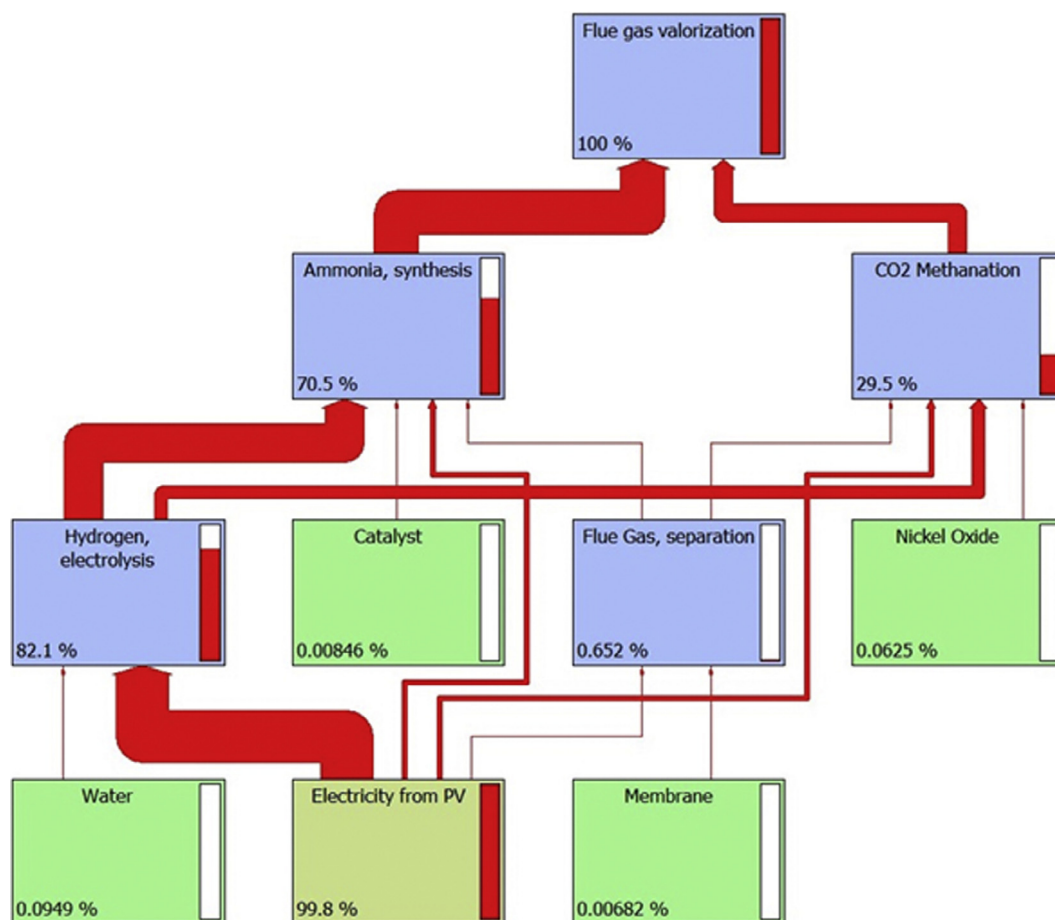
Fig. 7. Network view of CF results.

sustainability of the proposed process and its possible classification as a carbon recycling strategy to close the loop of CO_2 and, at the same time, put back carbon neutral fuel into the system.

4. Conclusions

In this paper, the authors propose a novel path to treat flue gas, in which H_2 production from electrolysis is integrated with ammonia production from N_2 by Haber-Bosch process and CH_4 production from CO_2 by Sabatier reaction.

PtG when combined with CO_2 and N_2 capture and storage technologies can be seen as a double solution: to provide energy supply and, at the same time, to put back into the industrial cycle further raw

Table 8
Carbon and Energy Footprint considering Italian Energy mix.

Phase	Carbon footprint		Energy footprint	
	(kg_{CO2eq} $kg_{fluegas}^{-1}$)	(kg_{CO2eq} kg_{H2}^{-1})	(MJ $kg_{fluegas}^{-1}$)	(MJ kg_{H2}^{-1})
NH_3 synthesis	0.9302	4.773	39.93	204.9
CO_2 Methanation	0.6197	3.180	19.19	98.48
Flue gas treatment	1.550	7.954	59.12	303.4

Table 7
Carbon and energy footprint.

Phase	Carbon footprint			Energy footprint		
	(kg_{CO2eq} $kg_{flueGas}^{-1}$)	(kg_{CO2eq} kg_{H2}^{-1})	(%)	(MJ $kg_{flueGas}^{-1}$)	(MJ kg_{H2}^{-1})	(%)
CO_2 Methanation	0.2305	1.183	29.48	14.94	76.65	29.45
Catalyst	0.0004890	0.002509	0.06	0.006698	0.03437	0.01
Flue gas separation	0.001439	0.007384	0.18	0.09280	0.4762	0.18
Electricity PV	0.0681	0.3494	8.71	4.4230	22.70	8.72
H_2, electrolysis	0.1605	0.8235	20.52	10.42	53.45	20.53
NH_3 Synthesis	0.5514	2.830	70.52	35.79	183.6	70.55
Catalyst	6.612E−05	3.393E−04	0.01	9.058E−04	0.004648	0.00
Flue gas separation	0.003663	0.01880	0.47	0.2362	1.212	0.47
Electricity PV	0.06626	0.3400	8.47	4.304	22.09	8.49
H_2, electrolysis	0.4814	2.5	61.57	31.25	160.3	61.60
Flue gas treatment	0.7819	4.012	100	50.73	260.3	100

materials flow for other kind of production purposes.

The process is studied through a LCA approach to determine carbon and energy footprint. Laboratory tests were performed to provide real data for CF and EF calculations. The reference functional unit is 1 kg of flue gas treated in input. The system boundaries include all the phases from production of input materials (reagents and water) and energy wares (electricity and H_2). The main results of the study are summarized hereunder:

- Results of experimental tests on CO_2 methanation section show a CO_2 conversion equal to 95.55% at 2.0 MPa.
- The total energy consumption per mass unit of flue gas is equal to 36,328 kJ_{el} and 186,418 kJ_{el} per mass unit of H_2. The electrolysis covers almost 80% of the electrical energy costs.
- From 1 kg of flue gas, 0.166 kg of CH_4 and 0.092 kg of NH_3 are produced.
- The total CF of the flue gas treatment process is 0.7819 kg_{CO2eq} $kg^{-1}_{fluegas}$, in case of electricity excess from renewable energy·NH_3 production is responsible of about 70% of the carbon footprint while CH_4 production is responsible of about 30%.
- The analysis was computed also in case of electricity from the grid, when the renewable electricity excess is not available. In this case, the total CF of the flue gas treatment process is 1.550 kg_{CO2eq} $kg^{-1}_{fluegas}$.
- In the face of a positive carbon footprint, the integrated production of synthetic CH_4 and NH_3 from flue gas indirectly leads to avoided emissions. The total amount of the avoided CO_2 emissions ranges from 0.673 to 0.844 kg_{CO2eq} $kg^{-1}_{fluegas}$ with an average value of 0.758 kg_{CO2eq} $kg^{-1}_{fluegas}$. This entails this process can be recommended to achieve carbon reduction targets by means of a CO_2 recycling strategy.

Acknowledgement

References

[1] European Parliament, Report on the implementation of the Circular Economy Plan, 2015. Available at < http://ec.europa.eu/environment/circular-economy/index_en.htm > (Accessed on May 16, 2018).
[2] Suda T, Fujii M, Yoshida K, Iijima M, Seto T, Mitsuoka S. Development of flue gas carbon dioxide recovery technology. Energy Convers Manage 1992;33:317–24.
[3] Bailera M, Lisbona P, Romeo LM, Espatolero S. Power to Gas projects review: Lab, pilot and demo plants for storing renewable energy and CO2. Renew Sustain Energy Rev 2017;69:292–312.
[4] Collet P, Flottes E, Favre A, Raynal L, Pierre H, Capela S, et al. Techno-economic and Life Cycle Assessment of methane production via biogas upgrading and power to gas technology. Appl Energy 2017;192:282–95.
[5] Parra D, Zhang X, Bauer C, Patel MK. An integrated techno-economic and life cycle environmental assessment of power-to-gas systems. Appl Energy 2017;193:440–54.
[6] Castellani B, Morini E, Bonamente E, Rossi F. Experimental investigation and energy considerations on hydrate-based biogas upgrading with CO2 valorization. Biomass Bioenergy 2017;105:364–72.
[7] Zhang X, Bauer C, Mutel CL, Volkart K. Life cycle assessment of power-to-gas: approaches, system variations and their environmental implications. Appl Energy 2017;190:326–38.
[8] Galindo Cifre P, Badr O. Renewable hydrogen utilisation for the production of methanol. Energy Convers Manage 2007;48:519–27.
[9] Castellani B, Gambelli AM, Morini E, Nastasi B, Presciutti A, Filipponi M, et al. Experimental investigation on CO2 methanation process for solar energy storage compared to CO2-based methanol synthesis. Energies 2017;10:855.
[10] Yoshida T, Tsuji M, Tamaura Y, Hurue T, Hayashida T, Ogawa K. Carbon recycling system through methanation of CO2 in flue gas in LNG power plant. Energy Convers Manage 1997;38:S443–8.
[11] Robinius M, Otto A, Heuser P, Welder L, Syranidis K, Ryberg DS, et al. Linking the power and transport sectors—Part 1: the principle of sector coupling. Energies 2017;10:956. http://dx.doi.org/10.3390/en10070956.
[12] Uusitalo V, Väisänen S, Inkeri E, Soukka R. Potential for greenhouse gas emission reductions using surplus electricity in hydrogen, methane and methanol production via electrolysis. Energy Convers Manage 2017;134:125–34.
[13] Gilbert P, Thornley P. Energy and carbon balance of ammonia production from

biomass gasification, Bio-ten., Holiday Inn, Birmingham, September 21–23; 2010. On line at: < https://www.escholar.manchester.ac.uk/api/datastream?publicationPid=uk-acman-scw:91274&datastreamId=FULL-TEXT.PDF > .
[14] Bicer Y, Dincer I, Zamfirescu C, Vezina G, Raso F. Comparative life cycle assessment of various ammonia production methods. J Cleaner Prod 2016;135:1379–95.
[15] Castellani B, Rinaldi S, Bonamente E, Nicolini A, Rossi F, Cotana F. Carbon and energy footprint of the hydrate-based biogas upgrading process integrated with CO2 valorization. Sci Total Environ 2018;615:404–11.
[16] Xu X, Song C, Wincek R, Andresen JM, Miller BG, Scaroni AW. Separation of CO2 from power plant flue gas using a novel CO2 "Molecular Basket" adsorbent. Fuel Chem Div Preprints 2003;48:162.
[17] Holladay JD, Hu J, King DL, Wang Y. An overview of hydrogen production technologies. Catal Today 2009;139:244–60.
[18] Castellani B, Rossi F, Filipponi M, Nicolini A. Hydrate-based removal of carbon dioxide and hydrogen sulphide from biogas mixtures: experimental investigation and energy evaluations. Biomass Bioenergy 2014;70:330–8.
[19] Aaron D, Tsouris C. Separation of CO2 from flue gas: a review. Sep Sci Technol 2005;40:321–48.
[20] Ahmad F, Lau KK, Lock SSM, Rafiq S, Khan AU, Lee M. Hollow fiber membrane model for gas separation: process simulation, experimental validation and module characteristics study. J Ind Eng Chem 2015;21:1246–57.
[21] Songolzadeh M, Soleimani M, Ravanchi MT, Songolzadeh R. Carbon dioxide separation from flue gases: a technological review emphasizing reduction in greenhouse gas emissions. Sci World J 2014, Article ID 828131, 34 pages, 2014. https://doi.org/10.1155/2014/828131.
[22] Powell CE, Qiao GG. Polymeric CO2/N2 gas separation membranes for the capture of carbon dioxide from power plant flue gases. J Membr Sci 2006;279:1–49.
[23] Moghadassi A, Marjani A, Shirazian S, Moradi S. Gas separation properties of hollow-fiber membranes of polypropylene and polycarbonate by melt-spinning method. Asian J Chem 2011;23:1922–4.
[24] Robb WL. Thin silicone membranes-their permeation properties and some applications. Ann N Y Acad Sci 1968;146:119–37.
[25] Membrane Basics. Available online at: < https://www.permselect.com/membranes > (Accessed on November 27, 2017).
[26] Van Der Sluijs JP, Hendriks CA, Blok K. Feasibility of polymer membranes for carbon dioxide recovery from flue gases. Energy Convers Manage 1992;33:429–36.
[27] Zhao L, Riensche E, Menzer R, Blum L, Stolten D. A parametric study of CO2/N2 gas separation membrane processes for post-combustion capture. J Membr Sci 2008;325:284–94.
[28] Zhao L, Riensche E, Blum L, Stolten D. How gas separation membrane competes with chemical absorption in postcombustion capture. Energy Procedia 2011;4:629–36.
[29] Saba SM, Müller M, Robinius M, Stolten D. The investment costs of electrolysis – a comparison of cost studies from the past 30 years. Int J Hydrogen Energy, Available online 11 December 2017, ISSN 0360-3199.
[30] Schmidt O, Gambhir A, Staffell I, Hawkes A, Nelson J, Few S. Future cost and performance of water electrolysis: an expert elicitation study. Int J Hydrogen Energy 2017;42:30470–92.
[31] Schiebahn S, Grube T, Robinius M, Tietze V, Kumar B, Stolten D. Power to gas: Technological overview, systems analysis and economic assessment for a case study in Germany. Int J Hydrogen Energy 2015;40:4285–94.
[32] Maslovara SL, Miulovic SM, Kaninski MPM, Tasic GS, Nikolic VM. Energy consumption of the electrolytic hydrogen production using Zn–Co–Mo based activators—Part I. Appl Catal A 2013;451:216–9.
[33] Nel Hydrogen; 2017. Available at < http://nelhydrogen.com/product/electrolysers/ > (Accessed on November 12).
[34] Di Profio P, Arca S, Rossi F, Filipponi M. Comparison of hydrogen hydrates with existing hydrogen storage technologies: energetic and economic evaluations. Int J Hydrogen Energy 2009;34:9173–80.
[35] Appl M. Process steps of ammonia production, in ammonia: Principles and industrial practice. Weinheim, Germany: Wiley-VCH Verlag GmbH; 1999.
[36] Frattini D, Cinti G, Bidini G, Desideri U, Cioffi R, Jannelli E. A system approach in energy evaluation of different renewable energies sources integration in ammonia production plants. Renew Energy 2016;99:472–82.
[37] International Fertilizer Industry Association (IFA). Energy Efficiency and CO2 Emissions in Ammonia Production 2008–2009 Summary Report Available at http://www.inference.org.uk/sustainable/images/2009_tech_energy_efficiency.pdf [Accessed on November 12, 2017].
[38] Filipponi M, Rossi F, Rossi R. Use of molten carbonate fuel cell for CO2 capture. ECS Trans 2012;42(1):43–7.
[39] Zhang Y, Ji X, Lu X. Energy consumption analysis for CO2 separation from gas mixtures. Appl Energy 2014;130:237–43.
[40] Autorità di regolazione per Energia Reti e Ambiente. Delibera EEN 3/08. Available online at: < https://www.arera.it/it/docs/08/003-08een.htm# > [Accessed on 22 January 2018].
[41] Zhao L, Riensche E, Weber M, Stolten D. Cascaded membrane processes for post-combustion CO2 capture. Chem. Eng. Technol 2012;35:489–96.
[42] SimaPro Software. Available at < https://support.simapro.com/?c=Getting_Started%3AGS_All > [Accessed on 11 December 2017].
[43] ISO (International Standard Organization). ISO/TS 14067:2013 Greenhouse gases—carbon footprint of products—requirements and guidelines for quantification and communication. Geneva, Switzerland: International Organization for Standardization (ISO); 2013.
[44] ISO (International Standard Organization). ISO 14044:2006a environmental management—life cycle assessment—requirements and guidelines. Geneva, Switzerland: International Organization for Standardization (ISO); 2006.
[45] Ruddock J, Short TD, Brudenell K. Energy integration in ammonia production. Transactions on Ecology and the Environment 2003 vol 62, WIT Press, ISSN 1743-3541.